Hydrokinetic Energy Recovery in Wind-Assisted Warships

C Greenhough MEng MSc *University College London (UCL)*
T Smith PhD CEng MRINA *University College London (UCL)*

Corresponding Author Email:
christopher.greenhough.17@ucl.ac.uk
tom.smith.17@ucl.ac.uk

Synopsis

There is a pressing need for navies to 'go green', to meet stricter regulations, decrease dependence on volatile energy supplies, and increase ship autonomy. It is therefore desirable for the military to operate in a leaner energy fashion, minimising oil requirements as much as possible and increasing the use of domestic and renewable energy sources.

Wind-assistance has seen a resurgence of academic and commercial interest recently driven by stricter regulations on atmospheric pollution from ship engines, encouraging advancements in new wind-assistance technologies. However, the power available from the wind is sporadic, and the inability for active warships to 'follow the wind' makes reliance on wind a difficult task. Considering this, additional flexibility may be offered when capturing wind energy by combining wind-assistance and energy recovery, using the propeller acting as a hydrokinetic turbine with the generated output being connected to the ship's electrical power system. As such, during periods when the wind power exceeds the propulsion demand, the excess energy may be captured and stored.

Previous research indicated a good level of reduction in fuel consumption when using wind-assistance combined with hydrokinetic energy recovery via a fixed pitch propeller. It was identified that the maximum reverse power flow for a given ship speed is closely linked to the propeller blade angle. Exploiting this fact, this study develops the concept by considering a controllable pitch propeller, offering a greater level of flexibility and potentially increasing the maximum reverse power flow which may be achieved. Torque and thrust characteristics of a propeller are estimated for a propeller in a turbine configuration using numerical methods to give an indication of potential improvements to energy recovery when using a controllable pitch propeller over a fixed pitch propeller.

Keywords: Hybrid; PTI; PTO; Propulsion; Integration; Marine systems; CFD; CPP

1. Introduction

The Royal Navy is increasingly conducting Operations Other Than War (OOTW), such as patrols, counter-piracy and counter-smuggling, humanitarian aid, and escorts. While the necessity still exists to be able to operate in a high-threat situation, these non-war-fighting scenarios allow the ships to operate in a greener, more eco-friendly and fuel-efficient manner. Governments are reliant on the energy provided by other nations to support their own military, and the volatility of oil prices, reliance on individual or small groups of nations, and reducing oil reserves make this model of energy unsustainable in the long run (O'Rourke, 2006; Wang et al., 2021). It is therefore desirable for the military to operate in a leaner energy fashion, minimising oil requirements as much as possible and increasing the use of domestic and renewable energy sources (Gougoulidis, 2015).

Of the many options for energy efficiency technologies, wind power is often shown to have significant benefits to ships (Buckingham, 2010; Pawling et al., 2016). It has seen a resurgence of interest, similar to that seen in the 1970/80's, then caused by an oil embargo with the middle east, and today caused by growing concern for climate change. Where commercial vessels generally have well defined and relatively simple operational profiles, and possibly have the autonomy to alter course slightly if it offers a cheaper overall transit, naval vessels must remain prepared for high-threat situations and must often place tactical and strategic goals above fuel efficiency. The integration of wind-assistance may therefore be more easily facilitated in a naval vessel by offering additional flexibility in the manner in which it can be operated. To this end, hydrokinetic energy recovery may offer a way to compound the benefit provided by wind assistance, by allowing excess wind energy to be harnessed and stored for later use. This would be achieved by operating the propeller as a turbine when wind conditions are favourable, thereby allowing the propulsion system to generate power and maximise the benefit of the wind when suitable.

Figure 1 shows a mock-up of the intended solution, in this case using a commercially available wing kite (SkySails, 2021) on a Type 45 Destroyer (Shipbucket, 2018), and indicating the bi-directional flow of mechanical power at the propeller. Previous research has indicated that there are significant energy efficiency gains possible in a warship when combining hydrokinetic energy recovery with wind assistance and it was noted that reverse power flow is sensitive to pitch-to-diameter ratio, and therefore blade angle (Greenhough et al., 2022).
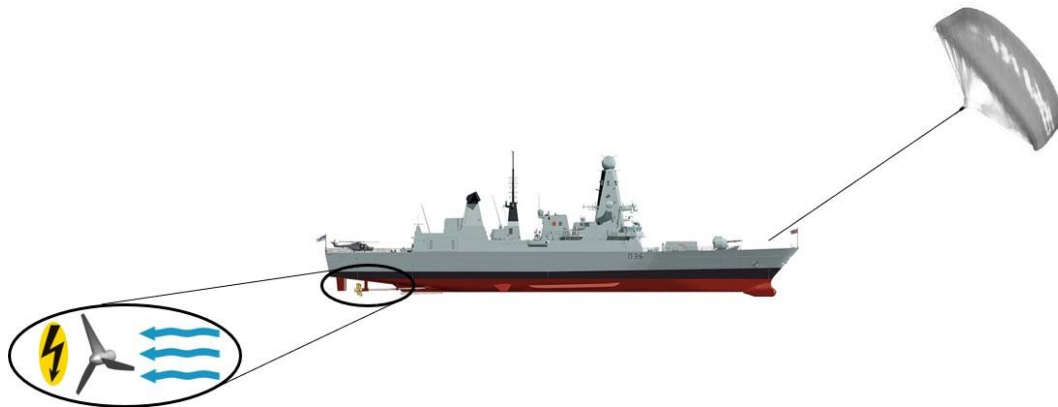
Figure 1 - Mock-up of Wind Assisted Warship with Hydrokinetic Turbine (Shipbucket, 2018; SkySails, 2022)

When a fixed pitch propeller operates in a turbine mode, the angle of attack experienced by the blades deviates from the design condition and potentially becomes negative. A more suitable configuration will see the blade section rotated about its centroid and the propeller permitted to rotate in the opposite direction, such that it causes a positive angle of attack when the ship is pulled through the water by a wind-assist device. The resultant force on the blade section will be more aligned with the propeller rotation and will increase the reverse power flow.

Data for propeller performance in this condition does not exist in the public domain, hence this work aims to generate such data using Computational Fluid Dynamics (CFD), by validating a model using known propeller performance characteristics, and then altering the blade angle to predict performance in a turbine configuration. Studies to predict the open water characteristics of propellers have been shown to give results commensurate with experiments (Islam & Jahra, 2019; M. A. Elghorab et al., 2013; Oloan et al., 2022), especially at lower values of advance coefficient (Saha et al., 2019). While similar research exists focused on controllable pitch propellers (Kolakoti et al., 2013), a bi-directional tidal hydrofoil (Nedyalkov, 2015), and a propeller with a camber-less blade profile instead of a controllable pitch propeller (Julià, 2019), no CFD modelling of a dual-mode propeller/turbine has been published.

This paper discusses the initial work to produce a CFD model which predicts propeller performance characteristics of a dual-mode controllable pitch propeller/turbine.

2. Propeller Characteristics

Systematic propeller testing has been conducted on a number of propeller designs, with the objective of creating a database which will support a designer in their decision making when it comes to propeller selection. One of the most widely tested and publicised datasets is that of the Wageningen B-Screw Series (Carlton, 2012). Given the extent of the available data, relationships have been defined that allow predictions of propeller torque, thrust, and therefore efficiency characteristics, across propellers of differing blade area ratios, blade numbers, and pitch-to-diameter ratios. It is trivial to estimate the performance characteristics of a propeller which falls into the range of characteristics which have thus far been tested. Table 1 shows the range of variables for which publicly available data is valid, with regards to the B-Screw Series.

Table 1 - Range of Tested Wageningen Propeller Series

	From	To
P/D	0.6	1.4
BAR	0.3	1.05
Z	2	7

During early-stage ship design, it is convenient to use propeller series data to predict propeller performance and allow propeller matching. Thrust and torque measurements from a range of propeller designs have been recorded and non-dimensionalised to give the Thrust Coefficient, K_t, and Torque Coefficient, K_q, as defined in Equation 1 and Equation 2, where T is propeller thrust, Q is propeller torque, ρ is density of water, n is propeller rotational frequency and D is propeller diameter. The non-dimensional speed is defined as the advance coefficient,

J, in Equation 3, where V_a is the ship speed of advance, and propeller efficiency, η, is predicted according to Equation 4.

$$K_t = \frac{T}{\rho n^2 D^4}$$

Equation 1

$$K_q = \frac{Q}{\rho n^2 D^5}$$

Equation 2

$$J = \frac{V_a}{nD}$$

Equation 3

$$\eta = \frac{T\,V_a}{2\pi nQ} = \left(\frac{K_t}{K_q}\right)\left(\frac{J}{2\pi}\right)$$

Equation 4

The propeller characteristics used in this study are largely commensurate with DTMB 5415 (Simman, 2008) however with a much-reduced blade area ratio to accommodate blade section rotation without self-intersection. It is noted that such a low blade area ratio is unlikely to be used in the suggested ship application, however, the model should still provide insight into dual-mode propeller/turbine operation.

Table 2 - Propeller Characteristics

Characteristic	Value	Units
Blade Number	4	-
Blade Area Ratio	0.3	-
Pitch/Diameter Ratio	1.4	-
Diameter	6.15	*m*

When operating in a turbine mode, the convention for relating fluid to blade speed is to use the Tip Speed Ratio, TSR, defined in Equation 5, where Ω is the propeller rotational speed in rad/s, and R is the propeller radius. The Power Coefficient C_p, the ratio of power extracted to power available, is defined in Equation 6, where A is the swept area of the propeller. In the context of turbine design, another value of interest is the Thrust Coefficient, which gives insight to the forces acting in the direction of fluid flow and therefore allows structural design to be considered. To avoid confusion with the propeller Thrust Coefficient, K_t, the term Drag Coefficient, C_d, will be used when considering the propeller acting in a turbine mode, and is defined in Equation 7.

$$TSR = \frac{\Omega R}{V_a}$$

Equation 5

$$C_p = \frac{Q\Omega}{\frac{1}{2}\rho V_a^3 A}$$

Equation 6

$$C_d = \frac{T}{\frac{1}{2}\rho V_a^2 A}$$

Equation 7

3. CFD Modelling

3.1. Geometry Modelling

Formulae conveying the coordinates of the blade section profiles give the non-dimensional positions of a number of points making up the blade profile (Oosterveld & van Oossanen, 1975). These outlines are created for each radial section, are then rotated to account for the pitch-to-diameter ratio, and then 'wrapped' around concentric cylinders at increasing distance from the hub, giving the propeller blade outline (Carlton, 2012). This blade is then 'locked' while being able to rotate about the z-axis, mimicking the movement of a controllable pitch propeller.

The face and back of each blade would join at an angle when applying the blade section formulae, which would cause challenges when meshing. As such, an edge thickness of 0.01% of the diameter is applied at the leading and trailing edges. Similarly, the blade is capped off at 99.5% of the radius to avoid infinitely thin sections. The hub/diameter ratio is 0.3, which is commensurate with a controllable pitch propeller, whereby the hub is generally larger to accommodate the additional machinery. The four-bladed propeller is modelled as one 90-degree angular section with periodic boundaries applied, reducing the computational effort significantly. The propeller centre has been defined by the intersection of the generator line of each blade section with the hub centre, from which measurements for the domain are referenced.
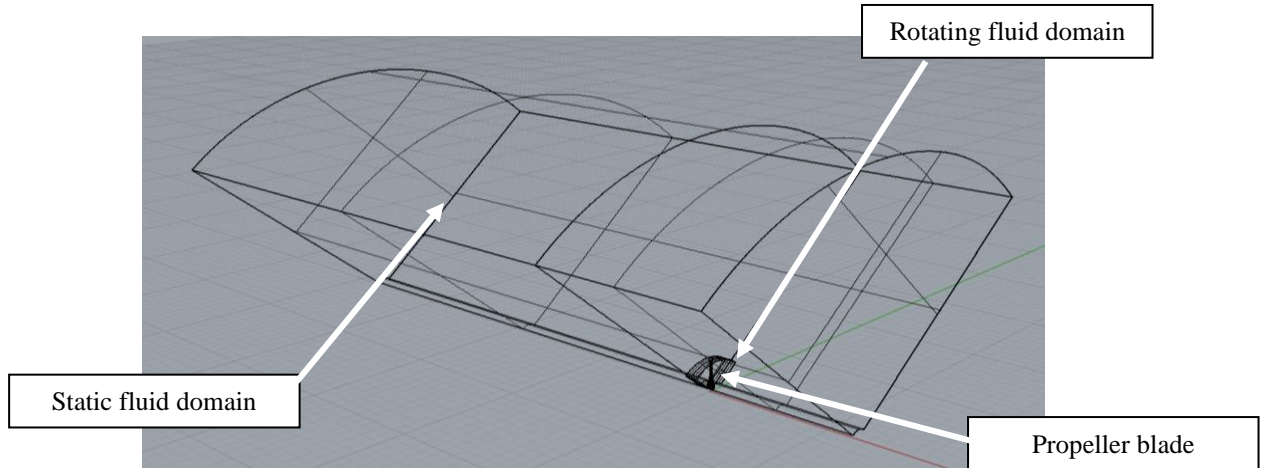

Figure 2 - Rhino model of propeller and fluid domain

3.2. Grid Generation

The commercial code ANSYS FLUENT R2022 (Ansys Inc., 2022) is used as the solver for this paper. The domain is modelled as a fluid (water-liquid), with single phase flow under steady-state conditions and using the SST k-ω turbulence model. To account for propeller motion in a steady-state simulation, a moving reference frame is assigned to the fluid domain immediately surrounding the propeller blade. The inlet speed is kept at 3 m/s for all simulations, with the rotational speed of the moving reference frame being changed to account for varying advance coefficients and tip speed ratios. The boundary conditions are stated in Table 3

Table 3 - Boundary Conditions

Boundary Name	Boundary Condition (FLUENT)
Inlet	Inlet
Outlet	Pressure Outlet
Radial wall	Symmetry
Propeller blade	Wall (no-slip)
Hub	Wall (no-slip)
Periodic boundaries	Periodic

The model is discretised using FLUENT MESHING (Ansys Inc., 2022), an automatic unstructured mesh generator which is built-in and integrated to the ANSYS FLUENT software. The volume mesh was generated using the FLUENT MOSAIC POLY-HEXCORE mesh feature. The domain dimensions were initially defined according to the recommendations of ITTC 7.5-03-03-01 (International Towing Tank Conference (ITTC), 2014). No suggestion is given regarding rotating domain sizing and so the axial and radial limits of the rotating fluid domain are set to 105% of the propeller dimensions in each direction for each blade configuration. Moving the inlet from 2D to 4D made negligible difference and so the former value was used. The outlet was moved from the recommended 4D to 6D as the wake pattern appeared to still be developing. The mesh is reasonably coarse in this region and so there was a minimal impact to computation time in doing so. The outer boundary in the radial direction was kept at the default value of 4D as there appeared to be no flow development and negligible impact on the results when increasing this value.

Refinement of the mesh was achieved with face size controls near the propeller blade, first boundary layer thickness and number of boundary layers, and maximum cell size all varied to build a grid independent model with

reasonable computation time. The mesh was required to have a minimum orthogonal mesh quality of at least 0.15 and the resultant mesh consisted of approximately 2.5M cells.

4. Results

Figure 3 shows the results of the CFD simulations of the propeller in the conventional propulsion configuration under typical propulsion conditions, as compared to the regressed experimental results of the Wageningen B-Screw Propeller Series. Table 4 shows the percentage error between the numerical results and the propeller series data. The data is qualitatively similar, although the numerical model underpredicts the torque and thrust coefficient. The efficiency also shows reasonable agreement throughout the range of advance coefficients, with a maximum error of 8.11%.
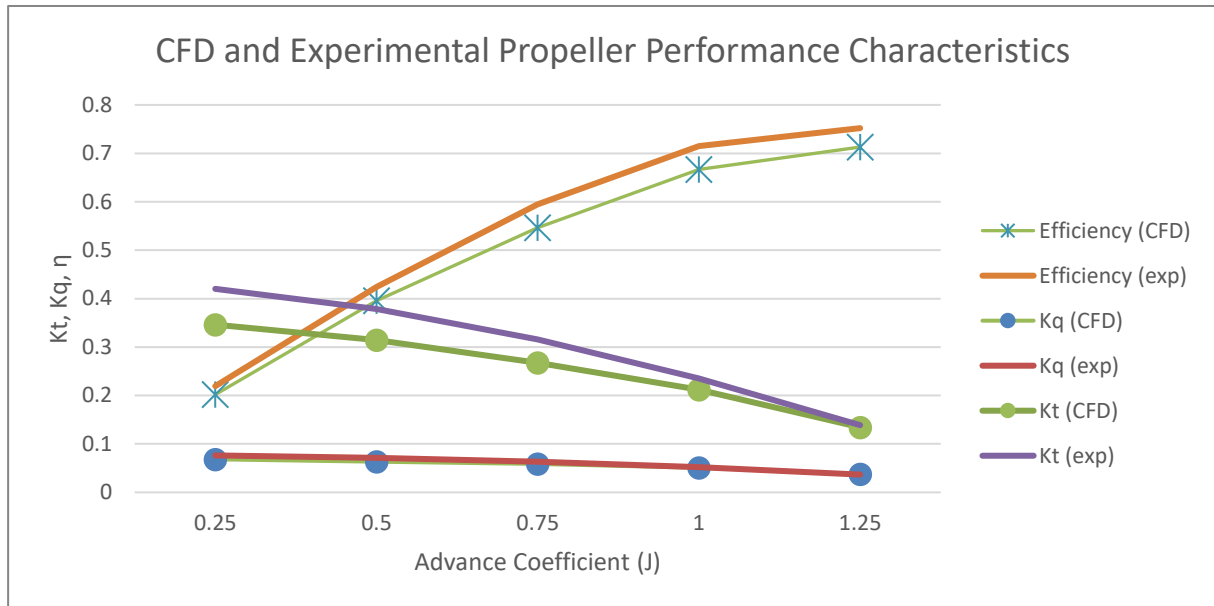

Figure 3 - CFD and Empirical Propeller Performance Characteristics

Table 4 - Percentage error between numerical and empirical results

Advance Coefficient	Torque Coefficient	Thrust Coefficient	Efficiency
0.25	10.53	7.19	7.91
0.5	10.91	7.48	6.73
0.75	7.67	11.30	8.11
1	3.26	8.49	6.78
1.25	2.11	4.50	5.19

To baseline the propeller performance in a turbine mode, the simulation is run with no changes to the propeller geometry and under regeneration conditions. Figure 4 shows the power coefficient and drag coefficient (right axis) and the ratio of power to drag coefficients (left axis). The maximum power coefficient of 0.016 occurs at a TSR of 1.25, while the maximum ratio of power-to-drag coefficients occurs at a TSR of 1.5, influenced by the substantially lower drag coefficient at this condition. Zero mechanical power at the propeller in propulsion configuration is found at a tip speed ratio of zero (i.e., the propeller is locked) and at a tip speed ratio slightly greater than 1.75, whereby the torque acting on the propeller is zero.
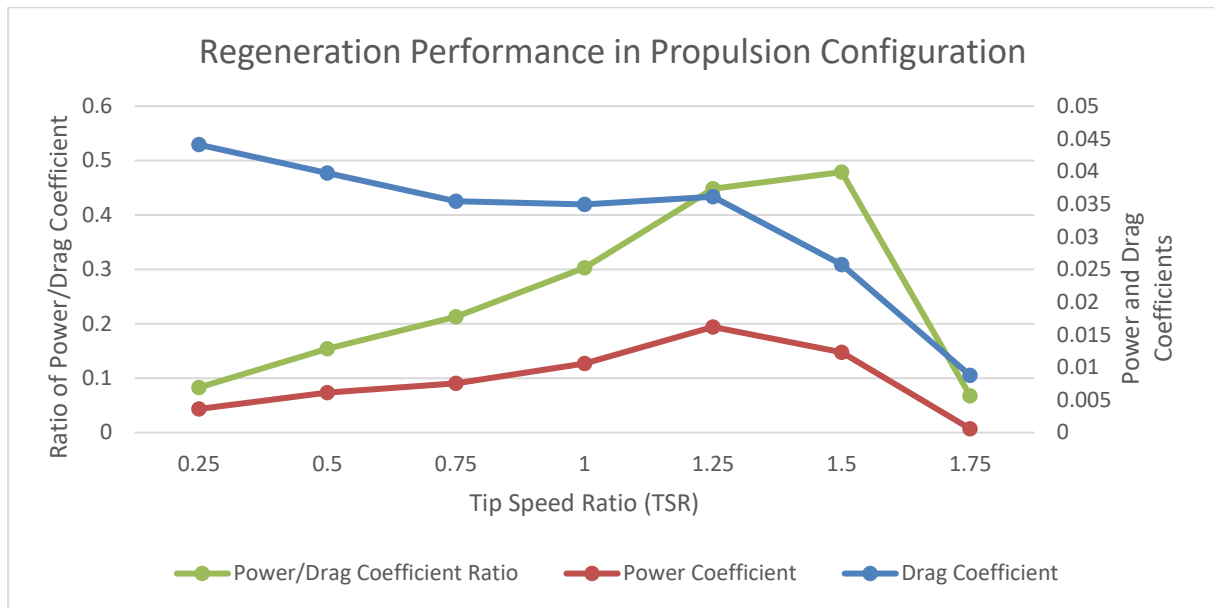
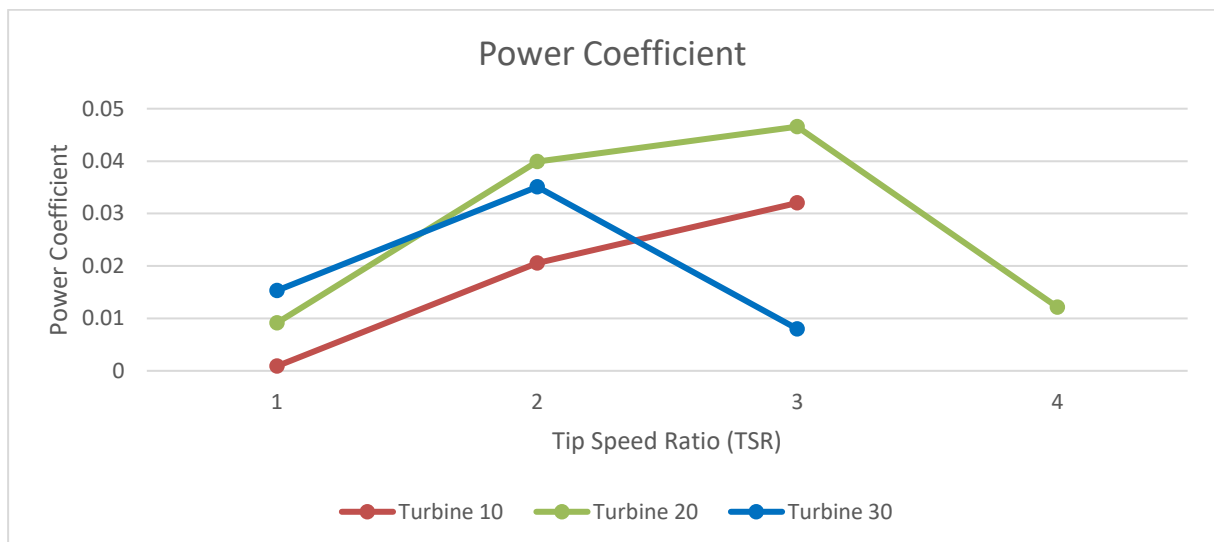Figure 4 - Regeneration Performance in Propulsion Configuration

Figure 5 - Power Coefficient in Turbine Configuration

Blade angle definition in the turbine configuration follows the convention of equalling zero degrees when the blade section nose-tail line at 70% of the propeller radius is colinear with the tangential velocity of the propeller and equalling 90 degrees when colinear with the ship direction of travel.

The effect on the power coefficient of altering the blade angle is shown in Figure 5. Only data points with reverse power flow at a TSR above 1 have been shown, i.e., blade angles of 40 degrees and above did not produce power above a TSR of 1. The power coefficient is seen to have a highly non-linear relationship with blade angle and a rapid reduction at higher values of TSR. The maximum power coefficient of 0.047, approximately three times greater than the maximum power coefficient in a propulsion configuration, occurs at a TSR of 3 with the blade angle at 20 degrees.

The drag coefficient for each blade angle configuration is shown in Figure 6, where it can be seen that increasing the blade angle reduces the drag coefficient, as higher blade angles bring the propeller closer to a feathered configuration, where lower drag is expected.

Figure 7 shows the ratio of power-to-drag coefficients for each blade angle configuration across the measured TSR range. The highest ratio of 0.38 occurs at a TSR of 2 for the 30-degree blade angle configuration. The next two highest ratios both occur in the 20-degree blade angle configuration at TSR of 2 and 3.
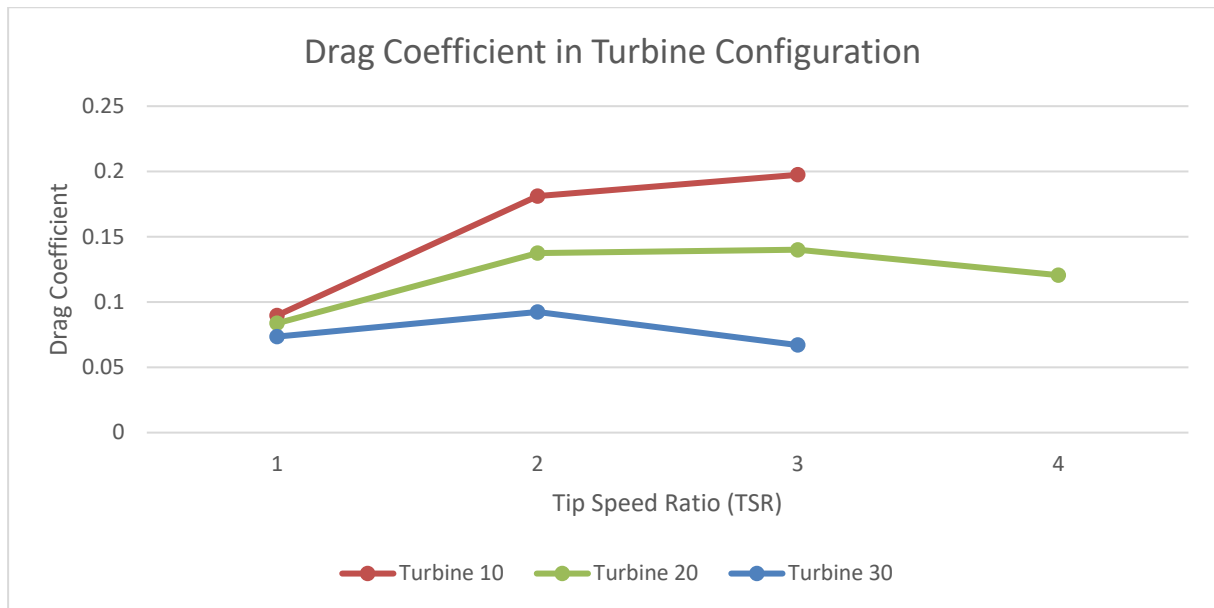
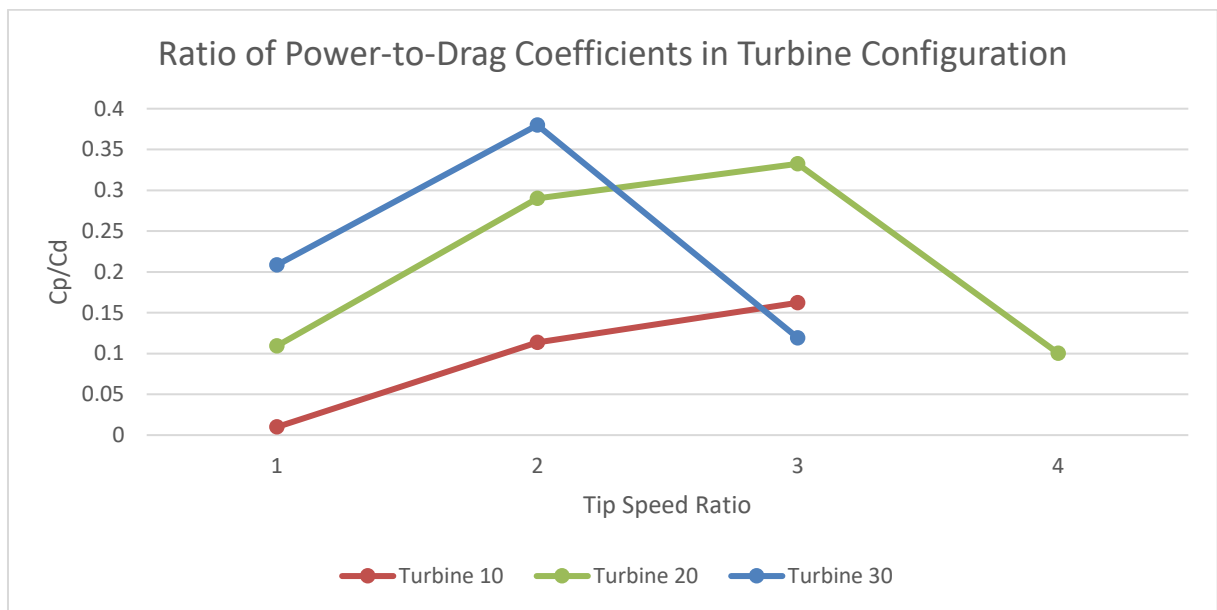Figure 6 - Drag Coefficient in Turbine Configuration

Figure 7 - Ratio of Power-to-Drag Coefficients in Turbine Configuration

The pressure distribution across the face changes between propulsion and turbine configurations, as shown in Figure 8, Figure 9, and Figure 10. The area of peak pressure in the propulsion configuration is towards the tip of the blade, while the turbine mode sees the peak pressure move toward the root of the blade, and to a greater extent with a higher blade angle. The turbine configuration also sees much lower pressures, with a maximum pressure of 46 kPa in propulsion mode and 11 kPa in the turbine mode.
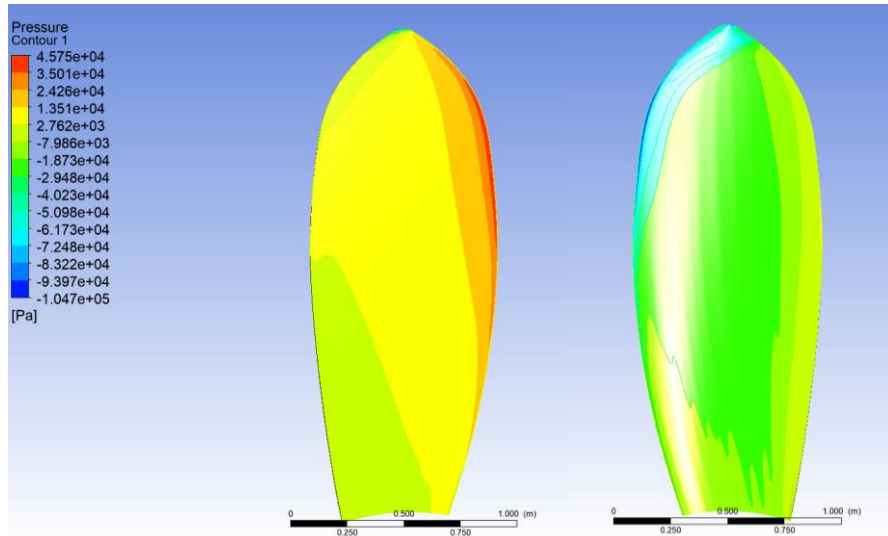
Figure 8 – Pressure Contour in Propulsion Mode – Blade Face (left) and Blade Back (right)
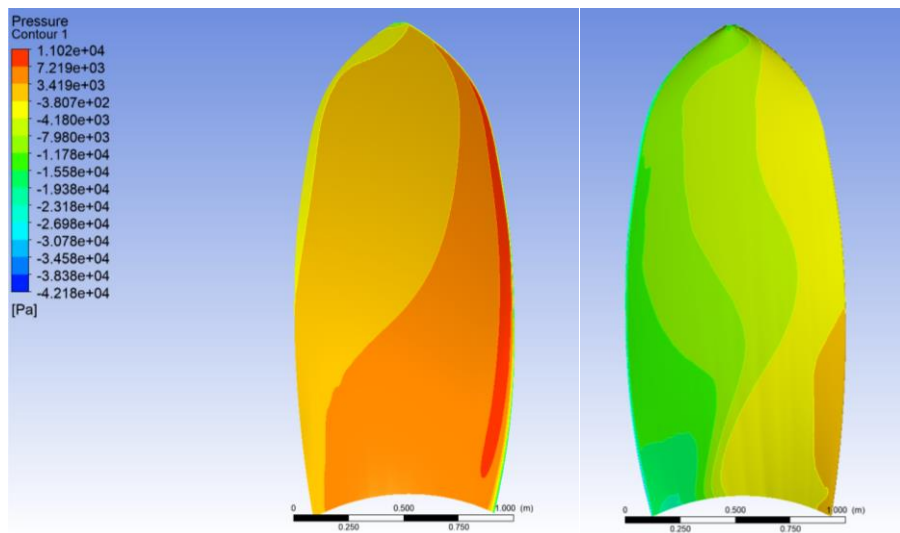

Figure 9 – Pressure Contour in Turbine Mode 20-degree at TSR = 2 - Blade Face (left) and Blade Back (right)
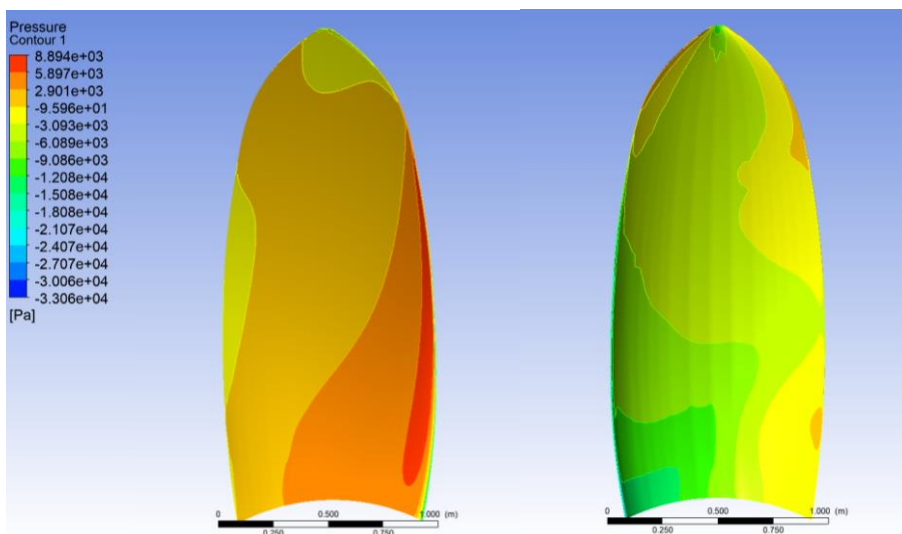

Figure 10 - Pressure Contour in Turbine Mode 30-degree at TSR = 2 - Blade Face (left) and Blade Back (right)

5. Discussion

The CFD model was found to have good agreement with the experimental data available, with an error that is comparable with other studies of a similar nature. Grid independence was achieved, suggesting the error is owing to geometrical differences between the simulated propeller and the experimental model, as well as the assumptions made, such as no free surface effect, single phase flow, and the loss of some transient effects when simulating a steady state. The hub-to-diameter ratio is also larger than is typical of fixed pitch propellers, and the torque and drag associated with the hub have been neglected from the measurements, which would likely result in lower values for both when compared to the experiments.

There is significant uncertainty when in regeneration mode as validating the simulations when operating in a turbine configuration is difficult owing to the lack of publicly available data to validate these conditions. While the good agreement of results in a propulsion configuration builds confidence, the more extreme flow patterns that can be expected suggest some neglected phenomena may have a greater impact in a turbine configuration, particularly flow separation. Towing tank tests on this type of configuration would be necessary to validate the model.

A higher power coefficient results in a greater proportion of the available hydrokinetic energy being captured by the turbine, however a lower drag coefficient suggests a higher ship speed for a given thrust provided by the wind, resulting in more hydrokinetic energy being available. It is therefore key to understand not only the power coefficient, as is the case in typical turbine applications, but also the ratio of power coefficient to drag coefficient, given that there should be minimal reverse thrust applied.

The propeller operates with a very low power coefficient in the propulsion configuration and within a small range of tip speed ratios. The drag coefficient is also very low in this configuration, which results in a reasonably high power-to-drag coefficient, indicating a reasonably low impact on ship speed.

The maximum power coefficient in the turbine configuration is approximately three times greater than in the propulsion configuration, suggesting the reorientation of the lift force with respect to propeller rotation has a significant impact on the possible reverse power flow. However, this is met with a significant increase in the drag coefficient when compared with the propulsion configuration, resulting in a lower overall power-to-drag coefficient ratio in the best turbine condition, compared to the propulsion configuration. As the resistance and the change of propeller thrust have highly non-linear relationships with ship speed, it is difficult to say if the higher power coefficient of a turbine configuration or higher power-to-drag coefficient ratio of propulsion configuration would be more beneficial to energy recovery overall and would depend on the contribution of propeller drag to total ship resistance.

Well designed turbines may operate at a power coefficient of between 0.3 and 0.4 (the Betz limit of 0.59 is never reached in practice), however this study suggests that assuming such a high value for dual-mode propeller/turbines may be very optimistic, overestimating reverse power flow by a factor of 10. It is noted that it remains unclear how sensitive the power coefficient is to blade characteristics, such as blade area ratio and pitch-to-diameter ratio when in propulsion mode.

It can also be said that, for a given ship speed, the propeller will experience lower stresses when in a generating mode than when propelling at that speed and may suggest that there is little additional structural consideration needed for dual mode propeller/turbines, as the pressure experienced in the turbine configuration is lower than in propulsion mode, and acts near the root where there is increased material.

6. Conclusion

In this paper, a CFD model was presented, comprising of a dual-mode propeller/turbine, validated in a propulsion mode against experimental data and then altered to a turbine configuration, such that the power coefficient and drag coefficient may be predicted. The simulation matched with the empirical data reasonably well, however it is difficult to confirm the validity of the results in the turbine configuration.

The turbine configuration resulted in an increase in maximum power coefficient by around a factor of three, however this was met with a similar increase in the drag coefficient. It is unclear if this will result in higher or lower reverse power flow, when considering the impact the drag will have on ship speed.

Following the indicative results of this paper, the CFD model will be validated against experimental data for a propeller in a turbine configuration and subsequently expanded to provide a wider range of turbine mode data to allow prediction of fuel savings during typical vessel operations.

References

Ansys Inc. (2022). *ANSYS FLUENT 2022 R1* (2022 R1).

Buckingham, J. (2010). Finding the right technologies to reduce fuel consumption. *RINA, Royal Institution of Naval Architects - Ship Design and Operation for Environmental Sustainability - Papers*, *January 2010*, 115–126.

Carlton, J. (2012). *Marine Propellers and Propulsion* (Third, Vol. 1). Elsevier.

Gougoulidis, G. (2015). Energy-saving Measures for Naval Operations. *6th Annual NMIOTC Conference 2015 Current and Future Challenges to Energy Security in the Maritime Environment*, *February*, 1–8.

Greenhough, C., Pawling, R., & Bucknall, R. (2022). Wind Propulsion: Operation with Hydrokinetic Turbine Energy Recovery. *14th Annual International Marine Design Conference* .

International Towing Tank Conference (ITTC). (2014). *ITTC - Recommended Procedures and Guidelines Practical Guidelines for Ship Self-Propulsion CFD*.

Islam, M. F., & Jahra, F. (2019). Improving accuracy and efficiency of CFD predictions of propeller open water performance. *Journal of Naval Architecture and Marine Engineering*, *16*(1), 1–20. https://doi.org/10.3329/jname.v16i1.34756

Julià, E. (2019). *Concept development of a fossil free operated cargo ship*. Chalmers University of Technology.

Kolakoti, A., Bhanuprakash, T. V. K., & Das, H. N. (2013). CFD Analysis of Controllable Pitch Propeller Used in Marine. *Global Journal of Engineering, Design and Technology*, *2*(5), 25–33.

M. A. Elghorab, Aly, A. A. E.-A., Elwetedy, A. S., & Kotb, M. A. (2013). *Propeller, Open Water Performance of a Marine CFD, Model Using*. *December*.

Nedyalkov, I. (2015). Performance and cavitation characteristics of bi-directional hydrofoils. In *PhD Thesis* (Vol. 1, Issue May). https://doi.org/10.1017/CBO9781107415324.004

Oloan, A. F. N., Made Ariana, I., & Baidowi, A. (2022). Open Water and Performance Analysis of Marine Propeller with PBCF Based CFD Method. *IOP Conference Series: Earth and Environmental Science*, *972*(1). https://doi.org/10.1088/1755-1315/972/1/012050

Oosterveld, M. W. C., & van Oossanen, P. (1975). Further Computer-Analyzed Data of the Wageningen B-Screw Series. *International Shipbuilding Progress*, *22*(251), 251–262. https://doi.org/10.3233/isp-1975-2225102

O'Rourke, R. (2006). Navy Ship Propulsion Technologies: Options for Reducing Oil Use - Background for Congress. *Defense*. https://www.fas.org/sgp/crs/weapons/RL33360.pdf

Pawling, R., Suarez de la Fuente, S., & Andrews, D. (2016). The Potential Use of Energy Saving Technologies in Future Patrol Combatants. *Warship 2016: Advanced Technologies in Naval Design, Construction, & Operation*, *June*, 15–16.

Saha, G. K., Maruf, M. H. I., & Hasan, M. R. (2019). Marine propeller modeling and performance analysis using CFD tools. *AIP Conference Proceedings*, *2121*. https://doi.org/10.1063/1.5115883

Shipbucket. (2018). *Destroyer Type 45 (Daring Class)*. http://shipbucket.com/forums/viewtopic.php?f=12&t=9081

Simman. (2008). *US Navy Combatant, DTMB 5415*. http://www.simman2008.dk/5415/combatant.html

SkySails. (2021). *Kite drive for yachts*. https://skysails-group.com/wp-content/uploads/2021/05/SkySailsYacht_Brochure_EN.pdf

SkySails. (2022). *SkySails - Information Pack*. https://skysails-group.com/wp-content/uploads/2022/01/SkySailsMarine_Brochure_EN_web.pdf

Wang, K. H., Su, C. W., Lobonţ, O. R., & Umar, M. (2021). Whether crude oil dependence and CO2 emissions influence military expenditure in net oil importing countries? *Energy Policy*, *153*. https://doi.org/10.1016/j.enpol.2021.112281